Continuum Models and Discrete Systems Symposia (CMDS-12) IOP Publishing
Journal of Physics: Conference Series **319** (2011) 012008 doi:10.1088/1742-6596/319/1/012008

The stationary flow in a heterogeneous compliant vessel network

Marcel Filoche
Physique de la Matière Condensée, Ecole Polytechnique, CNRS, 91228 Palaiseau, France

Magali Florens
CMLA, ENS Cachan, CNRS, UniverSud, 61 av. du Président Wilson, Cachan, France

Abstract. We introduce a mathematical model of the hydrodynamic transport into systems consisting in a network of connected flexible pipes. In each pipe of the network, the flow is assumed to be steady and one-dimensional. The fluid-structure interaction is described through tube laws which relate the pipe diameter to the pressure difference across the pipe wall. We show that the resulting one-dimensional differential equation describing the flow in the pipe can be exactly integrated if one is able to estimate averages of the Reynolds number along the pipe. The differential equation is then transformed into a non linear scalar equation relating pressures at both ends of the pipe and the flow rate in the pipe. These equations are coupled throughout the network with mass conservation equations for the flow and zero pressure losses at the branching points of the network. This allows us to derive a general model for the computation of the flow into very large inhomogeneous networks consisting of several thousands of flexible pipes. This model is then applied to perform numerical simulations of the human lung airway system at exhalation. The topology of the system and the tube laws are taken from morphometric and physiological data in the literature. We find good qualitative and quantitative agreement between the simulation results and flow-volume loops measured in real patients. In particular, expiratory flow limitation which is an essential characteristic of forced expiration is found to be well reproduced by our simulations. Finally, a mathematical model of a pathology (Chronic Obstructive Pulmonary Disease) is introduced which allows us to quantitatively assess the influence of a moderate or severe alteration of the airway compliances.

1. Introduction

Numerous transport networks, especially biological networks, can be modeled as a complex assembly of flexible pipes. This is for instance the case of the cardiovascular system in vertebrates (arterial and venous), of the lung airway system in mammals, and of the venation in plants (see figure 1). In all these networks, the overall flow is the result of the complex interplay between the applied pressures at the extremities and the non linear hydrodynamic resistances of the pipes. When large pressures are applied, the fluid-structure interaction induces non linearities that may lead to important inhomogeneities in the flow distribution. Local characteristics of the vessels then drastically affect the global flow distribution pattern across the network. The total flow is therefore a direct signature of both the topology of the network and the compliance of the pipes.

For large or inhomogeneous networks where analytical calculations are impossible to carry out, numerical simulations are a invaluable tool to obtain qualitative and quantitative predictions

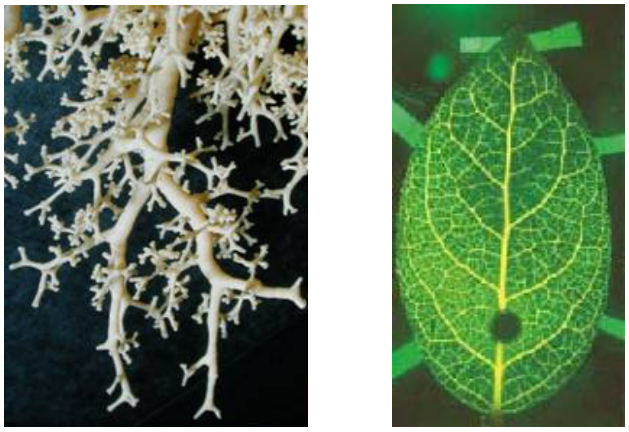

Figure 1. Left: Cast of the small airways of the human lung (E. R. Weibel). Right: venation of a leaf (S. Bohn, Rockefeller University, USA).

of the flow distribution for various working conditions, and to have a better understanding of the local and global features of these flexible networks [1]. Unfortunately, computing the flow in such systems requires in theory to solve the coupled equations governing the flow in the entire network of flexible pipes, and the 3D fluid-structure interaction in each pipe. This is in most cases out of reach for today's computing facilities.

We present here an alternative mathematical model that describes the flow into network through a large set of coupled equations, one for each flexible tube. First, we introduce a 1D model of the flow going through a single pipe. The fluid-structure interaction is modeled by state laws relating the local pipe diameter to the local transmural pressure. We then show that the 1D differential equation describing the flow in each pipe can be exactly integrated, provided one is able to estimate the average Reynolds number along the pipe. The 1D ODE in the pipe is then reduced to a scalar non-linear equation which relates the pressures at both ends of the pipe and the flow through the pipe. After adding Kirchoff laws at each node of the network to account for flow conservation, the entire flexible network is likened to an electrical network in which the unknowns are the pressures at the nodes of the network and the flow across the branches. Finally, this new model is applied to compute the flow in a specific case of particular interest, namely the lung airway system under forced expiration condition.

2. The 1D model of the flow through a flexible pipe

2.1. A differential equation for the transmural pressure

First, we assume a steady flow in the collapsible tube and steady pressures at both ends. Even in the case of an oscillatory flow, this simplification remains valid when the typical duration of a transient is small compared to the period of the cycle. The existence and the stability of solutions for the stationary flow in a collapsible tube has been examined and discussed in details in [2, 3, 4]. This assumption is for instance valid for most of the respiratory flow in the lung airway system [5].

Second, we consider that the flow is mostly one-dimensional along each pipe of the structure. The longitudinal coordinate along the tube is noted x. All the information about the cross-section is summarized into a position-dependent hydrodynamic diameter of the pipe, denoted $D(x)$.

Third, the fluid-structure interaction is modeled by a state law which relates the pipe diameter $D(x)$ to the local pressure difference across the pipe wall, also called *transmural pressure* P_{tm}.

This pressure is the difference between the local pressure P inside the pipe and the local pressure P_{out} outside the pipe: $P_{tm} = P - P_{out}$. The compliance of the tube is defined as the derivative of the state law with respect to the pressure. In most cases, this is a positive quantity which means that if the inside pressure exceeds the outside pressure, the transmural pressure is positive and the pipe opens. On the contrary if the transmural pressure is negative, the pipe tends to close. Figure 2 shows an example of a typical compliant behavior of a flexible pipe, i.e. two cross-sections of a pulmonary airway respectively under positive and negative transmural pressure.

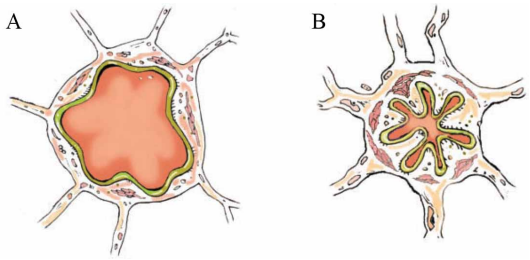

Figure 2. Typical behavior of a flexible pipe (here a bronchus) for two different values of the transmural pressure [6]. A: cross-section of the bronchus during inhalation, under positive transmural pressure. B: cross-section of the same bronchus during exhalation, under negative transmural pressure. One can observe the drastic reduction of the cross-section area hence the collapse of the hydrodynamic diameter.

The pressure profile is computed by solving in each pipe a 1D differential equation. For a steady and incompressible flow, the pressure at location x along the pipe is deduced from the pressure P_A at the pipe entrance (corresponding to the coordinate $x = 0$) using Bernoulli equation:

$$P(x) = P_A + \frac{1}{2}\rho\, v_A^2 - \frac{1}{2}\rho\, v^2(x) \; - \int_0^x f(y)\, dy \tag{1}$$

where P_A and v_A are respectively the pressure and the velocity of the flow at the pipe entrance, $v(x)$ is the velocity of the flow at point x, ρ is the fluid density, and $f(x)$ accounts for the energy loss per unit of distance. This last term always includes the viscous pressure loss per unit of distance and can also include a gravity term. The latter case is achieved by adding a constant term, equal to $(-\rho g \cos\theta)$ to $f(x)$, g being the acceleration due to gravity and θ the angle between the direction of gravity and the axis of the pipe.

If one assumes a uniform pressure in the medium surrounding the vessel network, then the transmural pressure P_{tm} also satisfies (1). The gradient of transmural pressure can be computed just by differentiating the above equation with respect to the coordinate x, and express the fluid velocity as a function of the flow rate Φ and the hydrodynamic diameter $D(x)$:

$$\frac{dP_{tm}}{dx} = -\rho v(x)\frac{dv}{dx} - f(x) = -\rho v(x)\frac{d\left(\frac{\Phi}{\pi D^2(x)/4}\right)}{dP_{tm}}\frac{dP_{tm}}{dx} - f(x) \tag{2}$$

This develops into:

$$\frac{dP_{tm}}{dx} = \rho v^2(x)\frac{2}{D(x)}\frac{dD}{dP_{tm}}\frac{dP_{tm}}{dx} - f(x) \tag{3}$$

Finally, the gradient of transmural pressure sums up:

$$\frac{dP_{tm}}{dx} = \frac{-f(x)}{1 - \dfrac{v^2(x)}{c^2(x)}} \qquad \text{with} \qquad \frac{1}{c^2(x)} = \frac{2\rho}{D(x)}\frac{dD}{dP_{tm}} \tag{4}$$

where $c(x)$ is the local wave speed.

For instance, the energy loss per unit of distance $f(x)$ can be evaluated in case of the bronchial network from Reynolds et al. [7]:

$$f(x) = \frac{128\eta\Phi}{\pi D^4(x)} \left(a + b\ Re(x)\right) - \rho g \cos\theta \tag{5}$$

where η is the fluid viscosity, $Re(x)$ is the local Reynolds number, and a and b are two phenomenological constants. The first term corresponds to viscous pressure loss per unit of distance; it is directly deduced from the experimental work of Reynolds et al [7]. The first part of this term corresponds to the viscous pressure loss for a Poiseuille flow. The constant a, which should be 1 for an infinite straight pipe, accounts for the fact that the Poiseuille profile needs some time to set up in the branches of the network. The second part of this term, characterized by a constant b, is a phenomenological term accounting for the loss when inertial effects are present, i.e. at higher velocities. In the following, we assume that the function $f(x)$ representing the energy loss per unit distance takes the general form (5) in our networks.

The denominator that appears in (4) corresponds to a negative feedback loop in the fluid-structure interaction that leads to flow limitation. It can be understood as follows. The dissipative pressure loss in the pipe tends to collapse the pipe which in turn generates an additional loss of transmural pressure by kinetic acceleration of the fluid. When the flow velocity is close to the wave propagation speed of a pressure disturbance along the pipe wall, the pressure loss increases causing the pipe to narrow even more. The resulting increase of the hydrodynamic resistance of the pipe automatically limits the flow rate. This mechanism has been described in details by Lambert et al. [8].

To sum up, the flow distribution in the network can be mathematically described by a set of differential equations, one for each pipe similar to (4). These equations are coupled by the continuity equations (Kirchoff laws) at each node of the network. Therefore, computing the flow in the entire network requires to solve in a coupled way as many differential equations as there are pipes in the network. Since biological networks usually correspond to several thousands of branches, this resolution is in most cases numerically unrealistic. To our knowledge, similar approaches have considered at most a few tens of flexible pipes in a network. Simulating large networks such as the lung airway system have been made possible only by assuming some sort of symmetry in the system. This allows one to solve only one differential equation per generation, this equation representing a large number of identical branches [8, 9, 5, 10, 11].

What we propose here is an alternative model based on an quasi analytical solution of the differential equation 4. After integration, each differential equation is transformed into a non linear scalar equation in which the unknowns are the transmural pressures at both ends of the pipe and the flow going through it. This will allow us to compute the flow distribution in the entire network, even in the case of large or non heterogeneous systems. We now describe this step.

2.2. Integrating the differential equation along a pipe

Starting from (4) one multiplies on both sides the equation by $\left(1 - v^2/c^2\right) D^4$ and then integrate between both ends of the pipe, noted A and B:

$$\int_A^B \left(1 - \frac{v^2(x)}{c^2(x)}\right) D^4(x)\ \frac{dP_{tm}}{dx}\ dx = -\int_A^B D^4(x)\ f(x)\ dx \tag{6}$$

This also expresses, using (5):

$$\int_A^B \left(1 - \frac{v^2(x)}{c^2(x)}\right) D^4(x)\ dP_{tm} = -\frac{128\eta\Phi}{\pi}\left[a\ L + b\int_A^B Re(x).dx\right] + \rho g\cos\theta\ \int_A^B D^4(x)\ dx \tag{7}$$

where L is the length of the pipe. Figure 3 shows a schematic representation of the flexible pipe and displays the various unknowns involved in the integration.

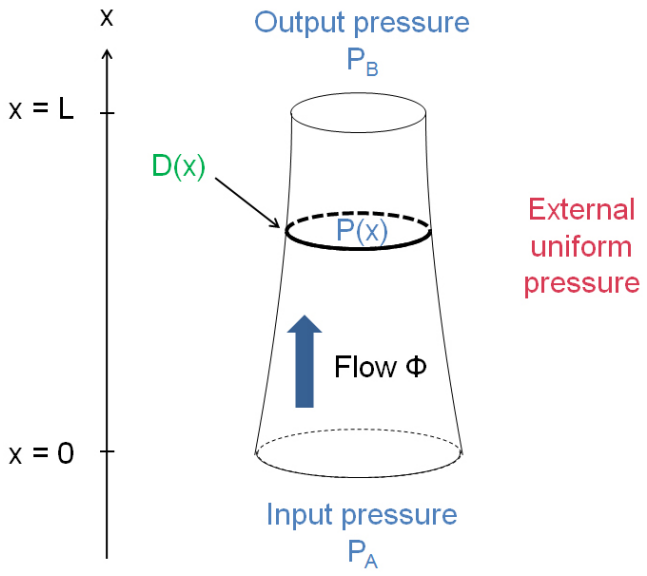

Figure 3. Schematic representation of the flow in one elementary flexible pipe of the network. L is the pipe length, $D(x)$ is the local diameter of the pipe at longitudinal coordinate x, P_A and P_B are the inner pressures at both ends of the pipes, and Φ is the flow rate going through the pipe. We recall here that the external pressure is assumed uniform.

The left hand side of (7) can be exactly integrated:

$$\int_A^B \left(1 - \frac{v^2(x)}{c^2(x)}\right) D^4(x)\ dP_{tm} = h(P_{tm,B}) - h(P_{tm,A}) - \frac{32\rho\Phi^2}{\pi^2} \ln\left(\frac{D_B}{D_A}\right) \tag{8}$$

where $P_{tm,A} = P_A - P_{out}$ (resp. B) is the local transmural pressure and h a function defined by: $h(P) = \int_0^P D^4(p)\ dp$. In other words, h is the primitive of the fourth power of the state law of the flexible pipe. The function $h(P)$ can be obtained from tabulated data or, when $D(P)$ is described by an analytical law as it is the case for instance in the airway system [8], it can even be an analytical function.

The right hand side of (7) writes:

$$-\frac{128\eta L\Phi}{\pi}\left[a + b\left\langle Re\right\rangle\right] + \rho g\cos\theta \int_A^B D^4(x)\ dx \tag{9}$$

where $\langle Re\rangle$ stands for the average Reynolds number along the pipe. The last term which requires to integrate D^4 can be rewritten using:

$$\Phi = \frac{\pi D^2(x)}{4}\ v(x) = \frac{\pi D^2(x)\eta}{4D(x)\rho}\ Re(x) \qquad \text{thus} \qquad D(x) = \left(\frac{4\rho\Phi}{\pi\eta}\right)\frac{1}{Re(x)} \tag{10}$$

which yields

$$\int_A^B D^4(x)\ dx = \left(\frac{4\rho\Phi}{\pi\eta}\right) L\ \left\langle Re^{-1}\right\rangle \tag{11}$$

Using (8) and (11), (7) finally writes:

$$h(P_{tm,B}) - h(P_{tm,A}) - \frac{32\rho\Phi^2}{\pi^2}\ln\left(\frac{D_B}{D_A}\right) = \\ -\frac{128\eta L\Phi}{\pi}\Big[a + b\left\langle Re\right\rangle\Big] + \rho g\cos\theta\ \left(\frac{4\rho\Phi}{\pi\eta}\right) L\ \left\langle Re^{-1}\right\rangle \tag{12}$$

As a result, in order to transform (12) into a scalar equation in which the only unknowns are the flow and the pressures at both ends of the pipes, one needs to compute the averaged quantities $\langle Re\rangle$ and $\left\langle Re^{-1}\right\rangle$ along the pipe. In most practical cases, both averages can be evaluated with a good precision using the average diameter of the pipe:

$$\langle Re^{\alpha}\rangle = \left(\frac{4\rho\Phi}{\eta\pi\left(\frac{D_S+D_E}{2}\right)}\right)^{\alpha} \tag{13}$$

One has to stress here that this approximation only affects the calculation of the dissipation in the tube and does not at all implicitly assume that the fluid velocity is constant along each pipe. We will see in the results section of the paper that this approximate calculation of the dissipation losses is justified. When applied to the lung airway system, it allows us to compute the stationary flow in the entire tree in a very good approximation at each stage of the breathing cycle.

In summary, we have transformed each differential equation describing the fluid-structure interaction in each pipe into a non linear scalar equation (12). Computing the flow through the network is now a feasible goal.

3. Computing the flow in the entire network

3.1. Continuity at the nodes of the network

When the entire network is considered, the scalar equations (12) describing the fluid-structure interaction in each pipe are coupled through Kirchhoff laws at each node of the network. Due to mass conservation at each node, the sum of the flow rates reaching a node is equal to zero. Also, the pressures at the ends of every pipe reaching the same node are supposed to be identical. This is equivalent to consider that the pressure losses are neglected in the branching region as compared to the pressure losses along the pipes.

$$\sum_{\text{branches } i} \Phi_i = 0 \qquad \text{and} \qquad \Delta P|_{branching} = 0 \tag{14}$$

The last assumption has been discussed for instance in the lung airway system by several authors [12, 13]. In the branching region, one can assume that the dissipative pressure losses are negligible since the transition from one branch to the next occurs on a short distance. Only the convective pressure losses could significantly contribute in the branching region. Furthermore, studies from the literature [14, 5] have shown no significant convective pressure drop occurring at the junctions. They are therefore neglected in our approach. These losses could nevertheless be taken into account in further studies by introducing a non-zero loss coefficient at the junctions as suggested by recent works [15, 1].

3.2. Boundary conditions and numerical scheme

In our model, the mathematical system describing the flow in the entire network consists in one scalar equation (12) per pipe, coupled by the Kirchoff laws described above at each node of the

network. The closure of this system is achieved by imposing boundary conditions at all exit nodes and branches of the network. The system can be pressure driven which means that the pressures are imposed at each exit node of the network. This is for instance the case for the lung airway system under forced expiration that we will present in the next section. The system can also be flow driven which means that the flow rates are imposed in all branches exiting the network. It can also be a combination of these two boundary conditions.

For a given set of boundary conditions, the non linear system is solved by an iterative Newton-Raphson scheme. As a result one obtains the flow rates and the pressures at both extremities for each pipe of the network, i.e. the flow distribution in the entire network. This also allows us to access the diameter and the pressure at any location x of each pipe, just by integrating (8) between one end of the pipe and this location.

The time-dependent response of a network such as the lung airway system is obtained using a quasi-static approach. At each time step of the expiration varying boundary conditions are applied at the extremities of the network. In the case of the lung airway system, the atmospheric pressure is applied at the mouth (which corresponds to the entrance of the system), and time-dependent alveolar pressures are applied at the distal ends of the tracheobronchial tree. The steady flow corresponding to these boundary conditions is then computed in the entire network. Finally, the time-varying response of the network is obtained from the sequence of these successive steady states.

4. Simulation results: the lung airway system

Several examples of compliant vessel network have been quoted in the introduction. We have chosen here to focus on a particular network, the lung airway system. The lung airway system in humans is a complex branched distribution system whose structure exhibits highly hierarchical features and scale invariance [16, 17, 18]. Ideally, this transport system is intended to deliver as uniformly as possible the flux of fresh air into the gas exchange units located in the distal regions. During inhalation the thoracic cage is lifted up and out by the respiratory muscles, leading to a natural opening of the pulmonary airways. On the contrary during exhalation the pressure exerted by the diaphragm and the elastic energy stored in the respiratory muscles tend to close the airways. The flow pattern in the tree is the result of a complex interplay between the flexible airway structure and the applied pressure distribution. In extreme conditions, as in forced expiration, the system exhibits non linearities that may lead to important inhomogeneities in the flow distribution. As a consequence, measuring the total flow rate out of the lung has become a routine clinical examination as a signature of the mechanical properties of the compliant bronchial geometry.

In the following, we study the lung airway system at forced expiration. First, the parameters of the model are detailed. Then, the results of the model are analyzed and compared to classical spirometric measurements made on patients.

4.1. Parameters of the model

The state laws giving the relationship between the local airway diameter D and the local transmural pressure P_{tm} are taken from the works of Lambert et al. [8]. The state law of any bronchus is defined with two analytical functions:

$$\begin{aligned} D(P_{tm}) &= D_{max}\sqrt{\alpha_0\left(1-\frac{P_{tm}}{P_1}\right)^{-n_1}} && \text{if } P_{tm}<0 \\ D(P_{tm}) &= D_{max}\sqrt{1-(1-\alpha_0)\left(1-\frac{P_{tm}}{P_2}\right)^{-n_2}} && \text{if } P_{tm}\geq 0 \end{aligned} \tag{15}$$

where D_{max} is the maximal diameter of the airway and α_0, n_1, n_2, P_1 et P_2 are adjustable parameters defining the flexibility or compliance of the airway. These parameters are tabulated in the paper of Lambert et al [8].

The energy loss per unit distance is defined by (5) in which the parameters a and b are respectively equal to 1.5 and 0.0035 in the lung airway system [7]. Since the fluid is air, gravity effects are negligible compared the viscous losses.

The lung airway system at exhalation is a pressure driven system. At the upper end (the mouth) the pressure is assumed to be constant and equal to the atmospheric pressure. At the extremities of the tracheobronchial tree, the pressure built by the respiratory muscles and the diaphragm output is called the alveolar pressure P_{alv}. Its time dependency is of exponential type, representing the relaxation of the lung towards equilibrium:

$$P_{alv}(t) = P_m(1 - e^{-t/\tau}) \left(\frac{V_L(t) - V_R}{C_V} \right) - R_T \Phi_0(t) \tag{16}$$

where P_m is the maximal pressure of the expiratory muscles, τ is the time constant of the expiratory muscles, V_L is the lung volume, V_R is the residual volume (the minimal functional lung volume), C_V is the vital capacity, R_T is the lung tissue resistance and Φ_0 is the flow rate in the first pipe of the network, here the trachea. All parameters in (16) are taken from the literature, tabulated for an healthy young adult [19, 20, 21, 22].

4.2. Spirometry of forced expiration

Forced expiration is simulated using the quasi-static approach described above. At each time step, a steady state of the lung airway system is computed: the flow, pressures and diameters of each airway are determined for a given set of pressure boundary conditions. In particular, the expiratory flow rate and the lung volume are calculated, allowing to obtain flow-volume loops. These loops plot the flow rate as an implicit function of the exhaled volume. Figure 4 displays flow-volume loops obtained for different patient's efforts. From A to C, the patient's effort decreases. This decrease is accounted for by changing the alveolar pressure P_{alv} through the parameters P_m and τ [23]. The computation time to retrieve a complete flow-volume loop is about one hour on a standard laptop for a lung airway system consisting in about 30,000 different bronchi.

First, the curves obtained from our simulations match real flow-volume loops measured on patients [24]. In the case A, the peak flow is about 10 L/s and the expired volume during the first second is about 4.6 L, which is in good agreement with typical measurements in healthy adults. Moreover, we recover the two characteristic parts of the flow-volume curve. The first part of the curve depends on the patient's effort: the peak flow increases for larger effort. The second part of the curve is independent of the patient's effort and linear with respect to the expired volume: air flow does not increase when the alveolar pressure increases. Recovering this characteristic twofold behavior is an important result that underlines the quality of the numerical model.

Using our set of simulations, one can try to assess the validity of the approximation made in (13). To that end, at each time step and for each airway we derive the local diameter $D(x)$ at each location along each airway using equation 12. From these data an *a posteriori* estimate of average Reynolds number in the airway is computed:

$$\langle Re \rangle = \frac{1}{L} \int_A^B \frac{4\rho\Phi}{\eta\pi D(x)} .dx \tag{17}$$

Our computations shows that the differences between the approximated and the exact average Reynolds numbers are most of the time about a few percents. They never exceed 20% in any of the airways, a value that is reached for a very short duration in only a small number of airways. This justifies in a self-consistent way the integration scheme chosen in (12).

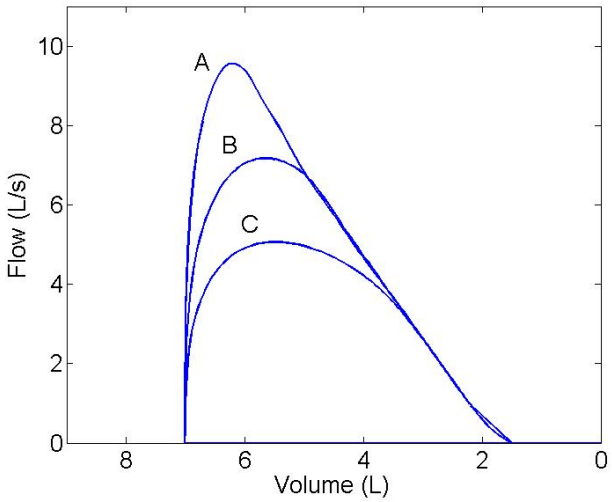

Figure 4. Flow-volume loops computed using a quasi-static computation of flow in the lung airway system. A: $P_m = 24$ kPa and $\tau = 0{,}2$ s; B: $P_m = 12$ kPa and $\tau = 0{,}3$ s; C: $P_m = 6$ kPa and $\tau = 0{,}4$ s [23].

4.3. Simulated pathology

After validation on healthy subjects, we now investigate the behavior of a pathological lung airway system under forced expiration. Several pathologies have been explored. The example presented here corresponds to a Chronic Obstructive Pulmonary Disease (COPD). COPD is a pulmonary disease characterized by an obstruction of the small airways. The alteration induces local and global modifications of the pulmonary mechanics. It is modeled in our case by introducing a local modification of the mechanical properties of the small airways. They become much more compliant due to a partial destruction of the surrounding parenchyma holding the airways. The elastic recoil forces also decrease so that the smallest airways are not completely open and tend to have a smaller diameter [25]. The global effects correspond to an increase of lung volumes [24], lung tissue resistance [21], and pulmonary compliance [26, 27].

Figure 5 displays the flow-volume loops simulated for an healthy airway system (A) and for two alteration levels (B and C). Both altered airway systems exhibit a reduced peak flow and a flow collapse after the peak flow as reported by West [24], and Pellegrino et al [28]. First, the decrease of the maximal diameters in small airways generates an increase of the airway resistance, which in turn induces a decrease of the expired flow. Secondly, the increase of both local and global pulmonary compliance leads to a more rapid collapse of the small airways. The dynamic compression of the small airways occurs faster and the expired flow drops sharply after the peak flow. One can observe in Figure 5 that this effect becomes even more important in the case of a severe alteration. All these simulation results are in very good agreement with the clinical observations.

5. Conclusion

In conclusion, we have derived a mathematical model which is capable of computing the flow distribution into a large heterogeneous network of flexible tubes. The fluid-structure interaction is introduced through state laws that relate the pipe diameter to the pressure difference across the pipe wall. After integration, the one-dimensional differential equations that govern the flow in each pipe of the network are transformed into a non linear system of scalar equations where

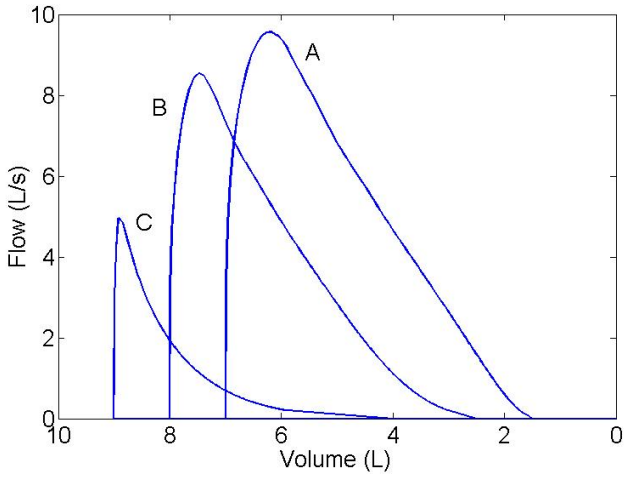

Figure 5. Flow-volume loops computed using our quasi-static model of the lung airway system. A: healthy airway system, B: moderate alteration of the airway system (moderate COPD), C: severe alteration of the airway system (severe COPD).

the unknowns are the pressures at each node of the network and the flow rates in each branch of the network. The system is closed by imposing boundary conditions at the exit nodes or in the exit branches of the network.

To assess its efficiency, this model has been applied to the human lung airway system. The topology of the vessel network and the compliance laws have been taken from the literature. This model allowed us to compute for the first time the response of a realistic asymmetric lung airway system at forced expiration, solving individually in each branch the flow rate during the entire expiration maneuver. The interest of this approach is that it permits to simulate large systems in a reasonable time, and to easily introduce morphometric or physiological modifications of the network in order to evaluate their influence on the global flow going through the structure. This approach is particularly fitted to understand the consequences of obstructive pathologies such as asthma or COPD at the local and global level during the breathing cycle in realistic bronchial trees. This could be used as a tool in a medical perspective to validate physiological hypothesis or to design new pulmonary function tests.

Finally, in the limit of a very dense network, one can think of combining the discrete equations (12) together with the mass conservation at each node to generate a continuous model of the flow through compressible porous media.

References

[1] Fullana J-M and Zaleski S 2009 *J. Fluid. Mech.* **621** 183-204
[2] Jensen O E and Pedley T J 1989 *J. Fluid. Mech.* **206** 339-374
[3] Elad D, Kamm R D and Shapiro A H 1989 *J. Fluid Mech.* **203** 401-418
[4] Kamm R D and Pedley T J 1989 *J. Biomech. Eng.* **111** 177-179
[5] Polak A G 1998 *Comput. Biol. Med.* **28** 613-625
[6] Tiddens H A W M, Donaldson S H, Rosenfeld M and Pare P D 2010 *Pediatr. Pulmonol.* **45** 107-117
[7] Reynolds D B 1982 *J. Biomech. Eng.* **104** 153-158
[8] Lambert R K, Wilson T A, Hyatt R E and Rodarte J R 1982 *J. Appl. Physiol.* **52** 44-56
[9] Isabey D 1982 *J. Biomech.* **15** 395-404
[10] Polak A G and Lutchen K R 2003 *Ann. Biomed. Eng.* **31** 891-907
[11] Barbini P, Brighenti C, Cevenni G and Gnudi G 2005 *Ann. Biomed. Eng.* **33** 518-530
[12] Pedley T J, Schroter R C and Sudlow M F 1970 *Respir. Physiol.* **9** 371-386

[13] Douglass R W and Munson B R 1974 *J. Biomech.* **7** 551-557
[14] Pardaens J, Van de Woestijne K P and Clement J 1972 *J. Appl. Physiol.* **33** 478-490
[15] Olufsen M S et al. 2000 *Ann. Biomed. Eng.* **28** 12811299
[16] Weibel E R and Gomez D M 1962 *Science* **137** 577-585
[17] Grotberg J B 1994 *Ann. Rev. Fluid Mech.* **26** 529-571
[18] Florens M and Sapoval B and Filoche M 2011 *J. Appl. Physiol.* **110** 756-763
[19] Agostini E and Fenn W O 1960 *J. Appl. Physiol.* **15** 349-353
[20] Weibel E R 1984 *The Pathway for Oxygen, Structure and Function in the Mammalian Respiratory System* (Cambridge: Harvard University Press)
[21] Verbeken E K, Cauberghs M, Mertens I, Lauweryns J M, Van de Woestijne K P 1992 *J. Appl. Physiol.* **72** 2343-2353
[22] Aguilar X, Fiz J A, Texido A, Vilalta P, Abad J, Richart C and Morera J 1996 *Respir. Med.* **90** 231-233
[23] Florens M and Sapoval B and Filoche M 2011 *Comput. Phys. Commun.* **189** 1932-1936
[24] West J B 2008 *Pulmonary Pathophysiology, The essentials, Seventh Edition* (Lippincott Williams & Wilkins)
[25] Guenard H and Rouatbi S 2002 *Rev. Mal. Respir.* **19** 230-240
[26] Greaves I A and Colebatch H J H 1980 *Am. Rev. Respir. Dis.* **121** 127-136
[27] Verbeken E K, Cauberghs M, Mertens I, Clement J, Lauweryns J M and Van de Woestijne K P 1992 *Chest* **101** 800-809
[28] Pellegrino R et al. J 2005 *Eur. Respir. J.* **26** 948-968